The interaction of shocks and defects in Lennard-Jones crystals

1993 J. Phys.: Condens. Matter 5 6357

(http://iopscience.iop.org/0953-8984/5/35/003)

J. Phys.: Condens. Matter 5 (1993) 6357–6376. Printed in the UK

The interaction of shocks and defects in Lennard-Jones crystals

Lee Phillips, Robert S Sinkovits, Elaine S Oran and Jay P Boris

Laboratory for Computational Physics and Fluid Dynamics, Naval Research Laboratory, Washington, DC, USA

Received 9 June 1992, in final form 7 May 1993

Abstract. We examine, using computational molecular dynamics, shocks launched in two-dimensional crystals by a flying plate. The interaction of the shock with various lattice defects is observed, and is seen to create sites of rapidly growing, thermalized, hot fluid-like phases included within the crystal lattice. We hypothesize that these fluid-like regions are the sites of the initial chemical reactions leading to detonation in energetic materials, and that crystallographic defects therefore control the sensitivity of single-crystal high explosives to shock-initiation. The computations are carried out on the massively parallel CM-200 using a parallelized version of the MLG algorithm.

1. Introduction

This paper investigates, on the molecular scale, the propagation of vibrational disturbances through various two-dimensional lattices, using the techniques of computational non-equilibrium molecular dynamics. These disturbances will be referred to as 'shocks', as is common in the literature, because, although they have a finite width and a definite structure, they are thought to be the microscopic analogues of the travelling discontinuities that are defined as shocks in the macroscopic domain of continuum mechanics.

The motivation behind the work reported in this paper is the desire to understand some of the peculiar properties of the initiation and propagation of detonations in solid chemical explosives. A detonation, as the term is usually understood in these contexts, is a physico-chemical process with a characteristic structure [1]. This structure consists, in a solid, liquid or gas, of a shock wave or some other localized traveling disturbance, followed by an associated reaction front, which separates material that has participated in a chemical reaction from material that is not yet reacted. The association between these two traveling interfaces, mediated by the 'induction zone' of (usually) compressed stressed unreacted material between them, is a complex interdependence whose nature has been the subject of many investigations, a few of which we shall discuss below. For now we should merely point out that, on the one hand, the shock is the cause of the reaction front, for in its passage it creates the conditions which lead to a particular series of reactions, while on the other hand the exothermic reaction front maintains and accelerates the shock by supplying kinetic and thermal energy.

In the fluid phases, those properties governing the nature of the detonation process are the chemical composition of the material along with its intensive thermodynamic variables and, sometimes, the details of the method used to initiate the detonation. In a solid, even when all of these quantities are held constant, there may still be significant variability in

0953-8984/93/356357+20$07.50

the responses of a series of samples. For example, in an experiment in which crystals are exploded by dropping a weight on them, the variability may take the form of a wide range of initial heights necessary for detonation in apparently identical samples. A possible source of this variable response might be some unknown and uncontrolled variation in the experimental conditions, presenting different samples with significantly different initial conditions, combined with an extreme sensitivity to initial conditions in the system. But it must be recognized that a sample of solid material, unlike a fluid, is characterized not only by its chemical composition and its thermodynamic state. The particular spatial arrangement of molecules constituting each sample makes them all unique. The fact that the shock, solitary compressional wave or other disturbance taking part in the structure of the detonation process is a mechanical mode of vibration supported by the molecular lattice, whose nature is completely dependent on the detailed structure of that lattice, implies that the spatial arrangement of molecules must influence the detonation process. This much is uncontroversial. What may be more surprising is the suggestion [2] investigated here, that certain minute changes in the molecular arrangement, involving the locations of just a few molecules, may have a large, even determining, effect on a macroscopic detonation. This suggestion gains plausibility if one considers that the actual thickness of the shock front may be only a few lattice planes [3]. Therefore the transfer of kinetic energy from a molecule to its neighbours in the direction of propagation involves the participation of only a few molecules (along the wavevector direction) in a particular vibrational mode at any one time.

One traditional theoretical approach to understanding detonations, and the initiation of a detonation by a shock wave, involves a description in terms of thermodynamic variables that are related by an equation of state for the material [1]. The passage of the shock heats the material through adiabatic compression; if the compression is great enough, then the local temperature will rise to a threshold required to initiate the chemical reactions, and a reaction front will form behind the shock. However, for understanding the detailed microscopic nature of detonations in a solid, the traditional theories may not be appropriate. At the scale of intermolecular distances, the usefulness of thermodynamic variables is problematic, and at timescales shorter than nanoseconds, relations built upon the assumption of thermodynamic equilibrium require special scrutiny (the rapid approach to thermal equilibrium under some circumstances is discussed further in section 3.) We should point out that a description based on classical mechanics, such as that employed here, must also be insufficient, but can form the basis for more accurate quantum or semi-classical descriptions.

In this paper we examine the point of view, championed by Walker [4–7], that a shock in a solid initiates detonation through the mechanical generation of scission forces on the molecules comprising the solid, breaking chemical bonds, creating a distribution of free radicals, and supplying the kinetic energy required to initiate reaction. In the light of this picture of the detonation process, we investigate the interaction of the shock front with the lattice structure, using numerical molecular dynamics. We are particularly interested in the effects of certain types of lattice defects on the shock initiation mechanism. We include no chemistry in our model; the 'molecules' are point particles interacting through Lennard-Jones potentials. Hence our current connection to the detonation problem is the exploration of how the conditions leading to the breaking of bonds and the subsequent formation of new molecules are established. The following stage, of reaction and shock acceleration, will be treated in a subsequent paper, which will report on simulations employing a chemistry model.

There have been reported a number of interesting molecular dynamics calculations that bear, in one way or another, on the problem of the shock initiation of detonations in solids. Karo and co-workers [8] simulated a small lattice of approximately one hundred

molecules arranged in a two-dimensional square-symmetric lattice, interacting through either 'endothermic' Morse potentials or 'exothermic' polynomial potentials. A shock was launched by simulating a flying plate consisting of a smaller lattice of identical construction to the main lattice. (This is quite similar to our method of shock launching in this paper.) The main conclusions were that the shock was quite narrow on the atomic scale, that the temperature of the lattice was unimportant, and that the free surface at the end of the finite lattice was a crucial feature, as the shock's interaction with this surface resulted in a spalling off of a large chunk of the crystal. The behaviour subsequent to the spalling depended on which potential was in use. With the endothermic potential there was little interesting activity after the separation of the chunk, but with the exothermic potential a violent reorganization of the lattice occurred.

While there is little reason to question the reliability of the general character of the results reported in these seminal papers, especially the importance of free surfaces, there are several numerical issues that should be discussed. Unfortunately, issues of convergence and accuracy are not treated in these references: conserved quantities are not mentioned, nor are the methods of integration. Instead of physically faithful additive potentials, the authors employ two different first- and second-neighbour potentials chosen to make the initial lattice stable. In addition, as the lattice undergoes its natural distortion and molecules acquire different sets of close neighbours, they are not allowed to interact with these new neighbours. Instead, the original table of bonds is used throughout the calculation. As the authors point out, this leads at times to molecules passing through each other without interaction. (Indeed, this is a statistical possibility, albeit of low likelihood [9], with the method we employ, as discussed below.) One of our goals in the work reported here is to discover which of these results survive the application of more modern numerical methods applied to somewhat more realistic simulations.

Later [10], using the same numerical method, these authors studied a shock in a lattice interrupted by a large gap consisting of a region with no molecules. As before, they observed spall from the free surface, with this time the spalled molecules reaching the second free surface beyond the gap and launching a second shock. This was an attempt to simulate efficiently the behaviour of a true void in a crystal, which would be surrounded by the lattice on all sides and make up a small fraction of the lattice. As we discuss in section 3, our simulations of small true voids included in a large lattice lead to somewhat different conclusions from simulations employing a gap.

In more recent related work, these authors and others [11–13] embed a computational surrogate for a polyatomic molecule into a simple host lattice, and show how the passage of the shock pumps energy directly into some of the vibrational modes of the molecule. This pumping could lead directly to bond scission in a real material, in a region that is definitely not ergodic, and where no thermodynamic temperature can be defined.

Also relevant is the work of Tsai and Trevino [14] on a diatomic perfect crystal in the form of a long filament with a small cross section. Exothermic bond breaking was simulated through the use of bound and free compound Morse potentials, and the shock was formed by heating the first six crystal planes. The initial temperature of their lattice was set at just below the threshold of spontaneous dissociation; the heating caused dissociation directly, the reaction spread by thermal conduction and drove a shock wave into the filament. They kept track of the stresses and examined the partition of kinetic energy in the induction zone, concluding that thermal equilibrium was not reached before dissociation took place. There is no discussion of numerical accuracy or the treatment of distant neighbours, although presumably the expediency of imposing a cutoff distance on the potentials, as adopted in a previous paper [15], was used here as well.

Several authors have demonstrated that the typical quasi-steady detonation structure described above is predicted by molecular dynamics models, with the exothermic reactive process modelled either by classical potentials acting between diatomic bonds [9, 16] or by a more elaborate procedure that captures some of the features of the quantum chemical processes involved [17–21]. All of these calculations involve perfect crystals, and although some of them examine the effects of lattice geometry, shock direction relative to lattice symmetry and so on, none of them deal with the action of crystallographic defects. A recent exception is the work of Maffre and Peyrard [22], which deals with the ability of a developed detonation structure to traverse grain boundaries, voids and other localized defects. However, they do not deal with the effect of defects in the transition from a pure shock to a detonation. Another exception is the recent work of Tsai [23].

2. Method

Our model system consists of an array of point particles, each with a specified initial position and velocity vector, arranged in a two-dimensional space with either periodic or free boundary conditions. The algorithms were chosen for their convenience and efficiency on the computer used, the Connection Machine CM-200, which consists of a large number (4096, 8192 or 16384, depending on configuration) of processors, each with its own set of locally stored data, updated in parallel according to instructions from a controlling 'front-end' computer. Efficiency consists here largely of maximizing the proportion of code that executes in parallel, which entails minimizing the manipulation of front-end (global) data and maintaining careful control over the pattern of communication among processors.

Forces between particles were represented by Lennard-Jones potentials. The solution of the complete N-body problem was not attempted; rather, the short-range nature of the Lennard-Jones potential was exploited to limit the distance over which interactions had to be computed. The particle data were distributed onto a data structure known as the monotonic Lagrangian grid (MLG) [24]. This is an object tracking and sorting technique where each particle is associated with a pair of integer indices i and j, and the assignment is ordered such that the coordinate x increases monotonically with i, and y increases monotonically with j. Monotonicity was enforced after each update in particle positions by a parallel version of the swapping routine described in [24]. The advantage of this method is that, at each timestep, a particle's neighbours can be identified quickly by cycling over a predetermined region of i–j space, rather than by searching through coordinate space with an expensive comparison of particle separations.

Each physical processor on the Connection Machine can be divided, in software, into as many virtual processors as memory will allow. When we refer to a 'processor' from here on, this should be taken to mean 'virtual processor'. One particle was associated with each processor, which stored the particle's position and velocity coordinates, as well as any other information unique to that particle. We also stored a near-neighbours template [24] in each processor; this is an array that stores the position information for each particle's neighbours in grid-index space. Once the template is filled, the total force vector acting on each particle and the update in position is computed for all particles entirely in parallel, with no additional interprocessor communication needed for the rest of the timestep. After each regeneration of the MLG by the swapping routine, the template is rebuilt; thus each processor–particle always has a locally stored updated list of the coordinates of its near neighbours. The use of the MLG is one of several available efficient schemes for replacing a time-consuming search for the spatially proximate neighbours of each particle at every timestep. However, as alluded

to in the section 1, its use can lead occasionally (but infrequently) to the problem of missed near neighbours [24], particles that are spatially close but not included in the neighbour template. In our calculations near-misses can always be detected by direct inspection of particle trajectories or by a failure of energy conservation or repeatability. In such cases we redo the calculation with a larger template. Thus the template size is treated like the computational timestep, both of which are adjusted to keep the calculations stable and accurate.

The procedure for filling up the template at each timestep is an important determinant of the overall efficiency of the algorithm. Interprocessor communication between neighbouring processors happens to be far more efficient than between more distant processors, so we fill the template using a sequence of coordinated data moves between neighbouring processors only. The total number of these parallel move operations is equal to one less than the total number of elements in the template array; therefore the total time required to fill the template depends on its size, not on the number of particles (assuming that the ratio of virtual processors to physical processors remains constant). Part of the communication sequence is diagrammed schematically in figure 1.

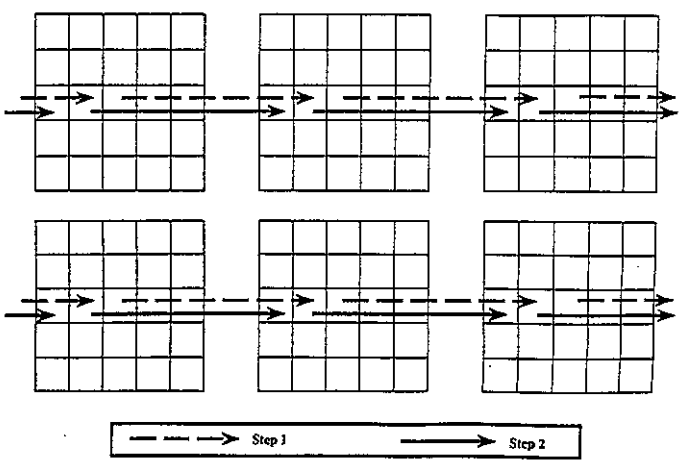

Figure 1. The two initial steps in a sequence of parallel move operations; the simplified case of a two-neighbour template is shown as an illustrative example, and the templates for six of the particles are included. Each processor's template is seeded at its centre with its own particle's data; the arrows represent the copying of particle data from a template entry to the appropriate template entry in a neighbouring processor.

As the studies described in this paper were being carried out, the computer hardware and system software being used was evolving. Fortunately, only one of these changes needs to be discussed here: initially, the Connection Machines that were used for these calculations were equipped with floating-point accelerators that operated only on 32-bit numbers; more recently, we were provided with 64-bit accelerators.

For reasonable efficiency, it is necessary to restrict the precision of floating point numbers to the word size of the accelerator. Therefore, some of the results reported here were performed with 32-bit arithmetic, some with 64-bit arithmetic, and some of the 32-bit calculations were redone with 64-bits (double precision) when that became available. The small differences we observed in particle data between the two precisions was not significant enough to affect our conclusions. The chief advantage to the greater precision will be for future calculations, which we will be able to carry out for longer times before the accumulated errors become unacceptable.

We found that single-precision arithmetic limited the accuracy with which energy can be conserved, and made the extra accuracy of higher-order time integration methods superfluous, and their use needlessly time-consuming. Therefore some of the results reported

here were calculated with the simple explicit Euler method. We were able to achieve stability with this method using a reasonable timestep. The consequence of the limitation of precision is that energy is conserved only to approximately one per cent in the 32-bit calculations. With double-precision arithmetic, it became advantageous to use a higher-order integrator. We have used both the leapfrog method (described in several places, for instance [25]) and the third-order Verlet formula [26] combined with a velocity corrector described by Beeman [27]. The advantage of this method (described on p 138 of [27]) is that the velocities do not have to be permanently stored, and need only be calculated when they are required for a data dump or a check of the kinetic energy. Our algorithm with these integrators can conserve energy to one part in 10^4, in actual calculations.

We have performed calculations with three different system sizes, 'small' grids of 2^{12} or 2^{13} molecules distributed among an equal number of physical processors, and a 'large' grid of 2^{15} molecules distributed among 2^{14} physical processors, which is the largest processor set available to us. (Our original machine, with two banks of 2^{12} processors, was replaced partway through this project with one of two banks of 2^{13} processors.) This 'large' system of particles is not very large by current standards of molecular dynamics simulation, but is adequate to demonstrate the physical processes of interest to us.

In both cases each molecule was assigned its own virtual processor. All else being equal, the large grid should take approximately twice as long to simulate as the small grids, because it is the ratio of virtual to physical processors that is significant. On the small grids, with five neighbours in the template in each direction, the calculation took 0.67 s per timestep. On the large grid, a five-neighbour calculation took 1.0 s per timestep and a seven-neighbour calculation took 2.0 s per timestep. We have verified several of our runs with equivalent calculations on the NRL Cray X-MP, using a well vectorized code. With 4096 molecules, a five-neighbour template takes 2–2.4 s per timestep; with larger system sizes, the disparity between the two architectures can be expected to grow dramatically [28].

3. Results

It is difficult to compare directly the various molecular dynamics simulations that can be found in the literature, due to the varying sets of units employed by different authors, along with differences in potential parameters, lattice spacing, initial conditions and so on, each of which can have a non-obvious effect on the evolution of the system. Close comparison becomes impossible when not enough parameters are supplied in order to characterize the dynamics of the system. In certain fields it is common to avoid these problems by describing the physical system with a set of dimensionless numbers. Although the large number of parameters characterizing a molecular system makes a simple resort to dimensionless numbers impossible, it may be useful to introduce one such number, which can be used to organize the results concerning the type of molecular dynamics configuration used in this paper.

We have an array of molecules with forces between them derived from a Lennard-Jones potential

$$\phi = 4\epsilon[(\sigma/r)^{12} - (\sigma/r)^6]$$

so the force, F, is given by

$$F = -\frac{\mathrm{d}\phi}{\mathrm{d}r} = 4\epsilon\left(-12\frac{\sigma^{12}}{r^{13}} + 6\frac{\sigma^6}{r^7}\right) = m\frac{\mathrm{d}^2 r}{\mathrm{d}t^2}$$

by Newton's equation of motion. In the above two equations r is the distance from the molecule, m is the molecular mass, t is time, and ϕ and ϵ are the two parameters characterizing the potential. In order to make the equation of motion dimensionless, we must introduce scales appropriate to a system excited by a flying plate: d is the interparticle spacing, V_p is the plate velocity, $\tau = d/V_p$, μ is the particle mass, and $\Sigma = \mu d^2/\tau^2$ is the energy unit.

After making the substitutions

$$r \to r'd \qquad \epsilon \to \epsilon'\Sigma \qquad t \to t'\tau \qquad m \to m'\mu \qquad \sigma \to \sigma'd$$

and removing the primes from the now dimensionless variables, the equation of motion becomes

$$\mathcal{L}^{-1}4(-12\sigma^{12}/r^{13} + 6\sigma^6/r^7) = m\frac{d^2r}{dt^2}$$

where

$$\mathcal{L} \equiv \frac{V_p{}^2\mu}{\epsilon}$$

emerges as a new dimensionless number, apparently relating the kinetic energy of the impacting molecules to the binding energy of the intermolecular potential.

In all of the calculations presented here, $\epsilon = 0.0223$, $\sigma = 0.891$, $V_p = 2.0$, $d = 1.0$, and $\mu = 4.0$, giving $\mathcal{L} = 727.3$. It may help put things into context for some readers if we scale our variables to the values appropriate to solid argon, a substance commonly discussed. In this case the plate velocity scales to $4258\,\mathrm{m\,s^{-1}}$, one time unit is 0.88×10^{-13} s, and one distance unit is 3.8 Å. From here on we shall use the dimensionless units.

Figure 2 shows a sequence of molecular configurations as a plate-launched shock encounters a pair of voids in a system with periodic boundaries transverse to the shock, producing a great deal of disorder. The same initial conditions in a system without the voids lead to the shock traversing the crystal intact and leaving it undisturbed. However, this behaviour is observed in the inherently unstable square lattice used for this run only at near-zero initial temperatures, in contrast with the stable hexagonal lattice used in other runs described below. We see here that the voids disturb the coherency of the shock, transforming its organized x-directed (horizontal) motions into a thermalized two-dimensional (x–y) motion; beyond the defects, the shock continues as several disconnected pieces.

The progress of the shock can perhaps be more clearly visualized in figure 3, showing profiles of the horizontal velocity along different lines through the crystal. That these disordered regions are actually 'thermalized' can be seen by looking at the speed distribution of the molecules in the crystal. Figure 4 is a series of speed histograms corresponding to the calculation illustrated in figure 2; superimposed on each histogram plot is the two-dimensional Maxwell–Boltzman distribution with a temperature derived from the average kinetic energy of all the particles. At early times we can see the speed distribution dominated by two values, the near-zero speed of the particles locked into the near-zero temperature lattice configuration, and the highest speed, equal to the plate velocity. As time advances we can see the velocity distribution filling in, but remaining non-Maxwellian. In the last frame of the figure we have plotted the distribution of a subset of the system at $t = 15$ (the configuration at this time is shown in figure 14), the subset consisting of the particles in the chaotic region delimited by $x = 15$ and $x = 42$. The superimposed Maxwell–Boltzman

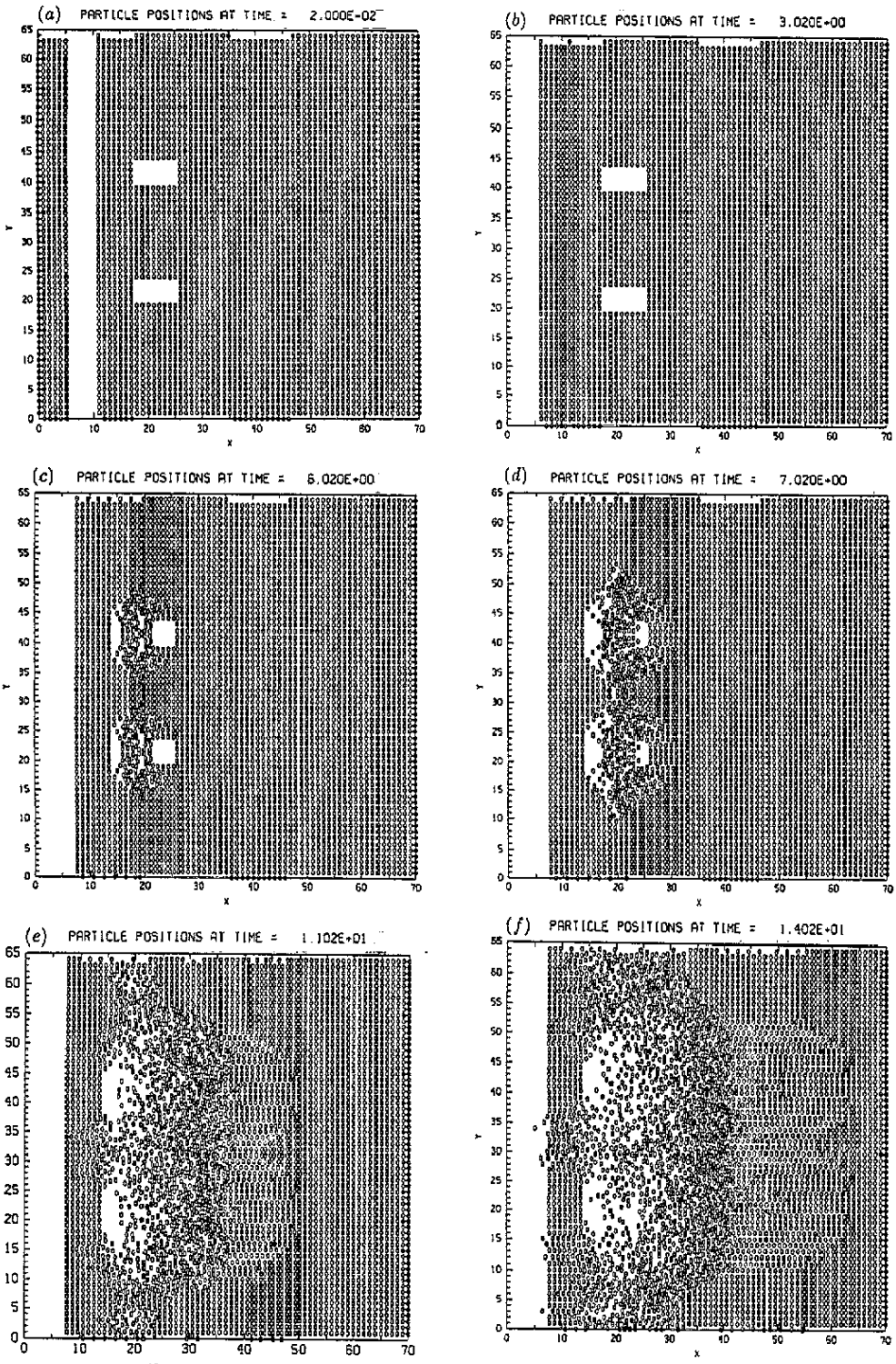

Figure 2. Particle positions for 4k particles in two dimensions, with periodic boundary conditions in the y direction. A 'flying plate' impinges from the left, and has just made contact at $t = 3$; the resulting shock, propagating in the x direction, interacts with two rectangular voids.

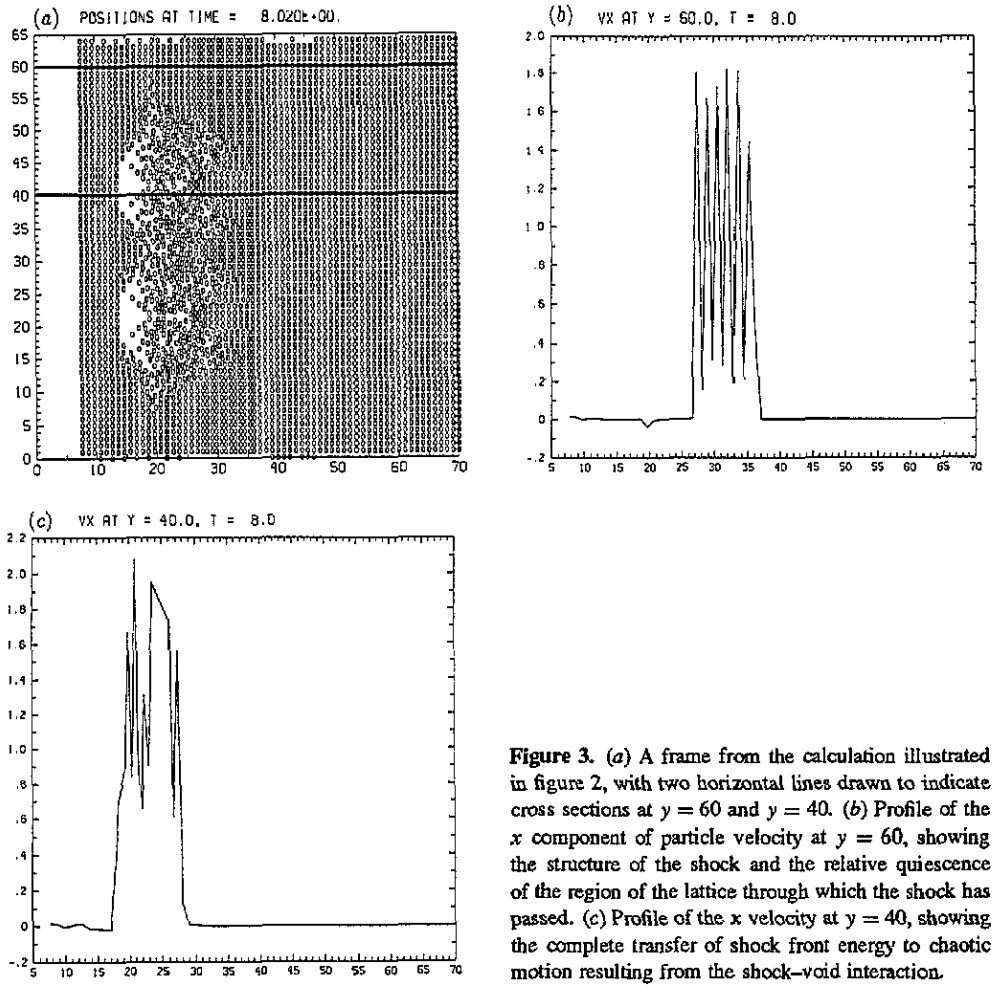

Figure 3. (*a*) A frame from the calculation illustrated in figure 2, with two horizontal lines drawn to indicate cross sections at $y = 60$ and $y = 40$. (*b*) Profile of the x component of particle velocity at $y = 60$, showing the structure of the shock and the relative quiescence of the region of the lattice through which the shock has passed. (*c*) Profile of the x velocity at $y = 40$, showing the complete transfer of shock front energy to chaotic motion resulting from the shock–void interaction.

curve corresponds to the kinetic temperature of the subset of particles under consideration; clearly this region of particles has rapidly attained a thermal equilibrium, indicating that the collisionality in the chaotic region is high. The creation of hot spots at the site of voids in a lattice under compression has also been seen in recent simulations by Tsai [23]. These disordered regions also have the property of being at a slightly higher density than the equilibrium lattice, as can be seen in the density plot of figure 6.

A similar calculation can be seen in figure 5, with the square lattice replaced by a hexagonal lattice. In this case, also, the small void has been replaced by a single vacancy. We can see here that even in a lattice geometry with a higher binding energy, and with, unlike the square lattice, non-linear stability against moderate temperatures, a small imperfection creates a large disruption.

It is important to keep in mind that the 'voids' (and hot spots) discussed here, and in related papers, are at a vastly different length scale from the voids (and hot spots) that can currently be observed in experiments, which are typically in the micron range, which is a huge expanse for a molecular dynamics calculation. As simulation length scales become larger, and laboratory observations become more minute, perhaps eventually there will be

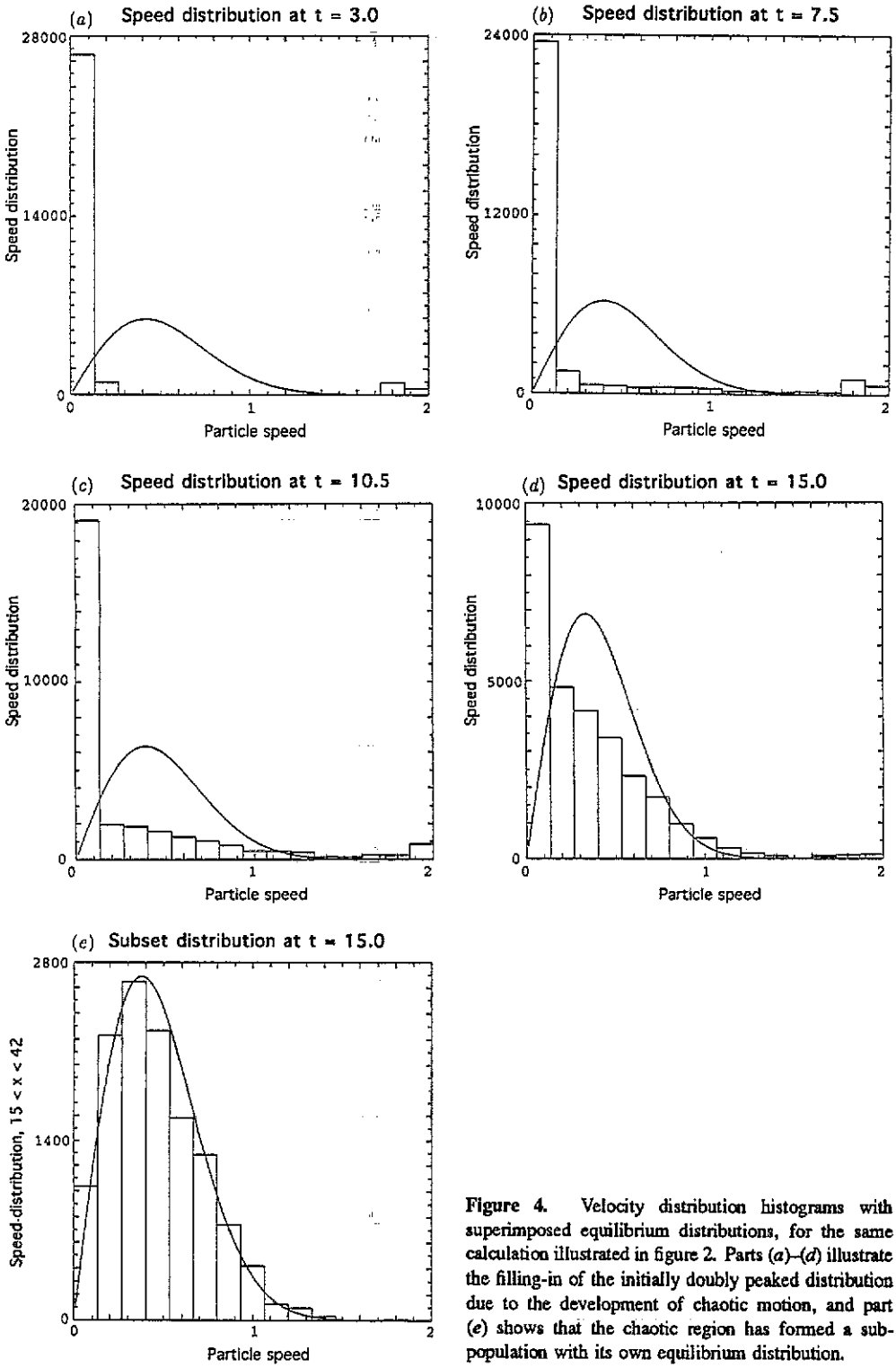

Figure 4. Velocity distribution histograms with superimposed equilibrium distributions, for the same calculation illustrated in figure 2. Parts (*a*)–(*d*) illustrate the filling-in of the initially doubly peaked distribution due to the development of chaotic motion, and part (*e*) shows that the chaotic region has formed a sub-population with its own equilibrium distribution.

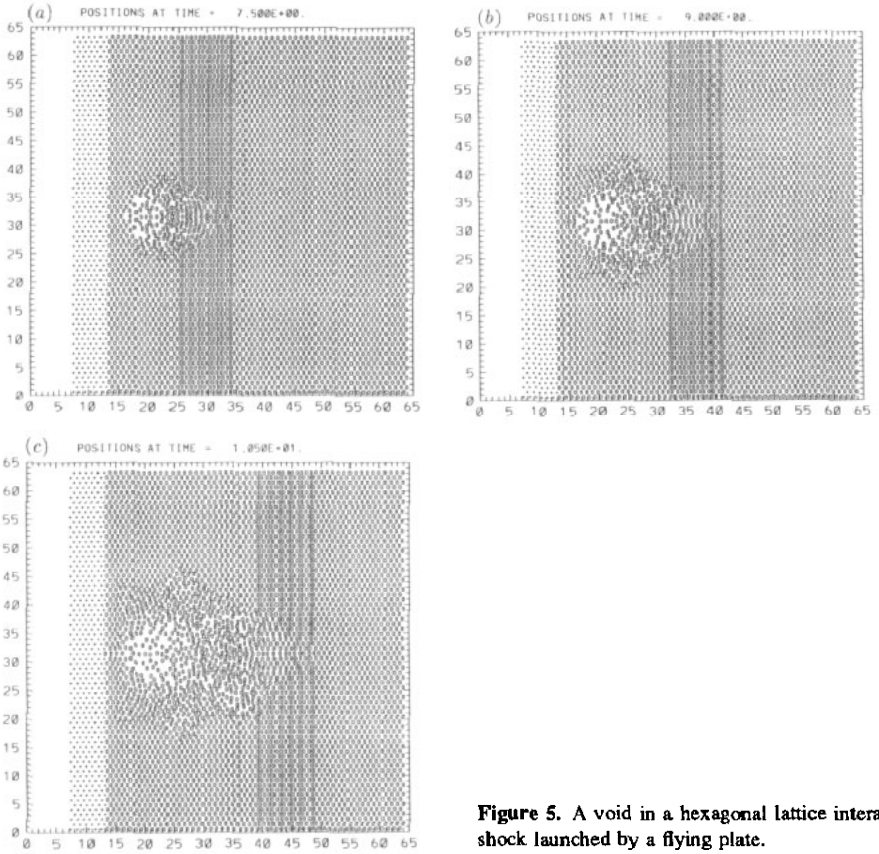

Figure 5. A void in a hexagonal lattice interacting with a shock launched by a flying plate.

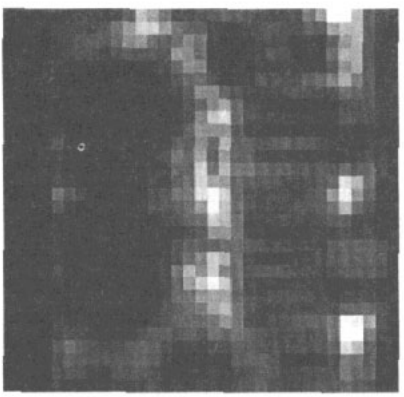

Figure 6. Smoothed density plot corresponding to the same calculation illustrated in figure 2, at $t = 13.5$. Increasing brightness indicates increasing density. The three bright patches near the right-hand side of the figure correspond to the compression at the location of the void-interrupted shock.

a closer connection between molecular dynamics and experiments.

The interaction of a shock front with a mass defect in square and hexagonal lattices can be seen in figures 7 and 8, both showing the effect of the inclusion of a molecule with a 50% mass excess. The effects are similar to but weaker than those caused by voids.

We have performed a series of experiments on systems identical to the ones shown in the figures, but at various temperatures and intermolecular potential well depths. At very

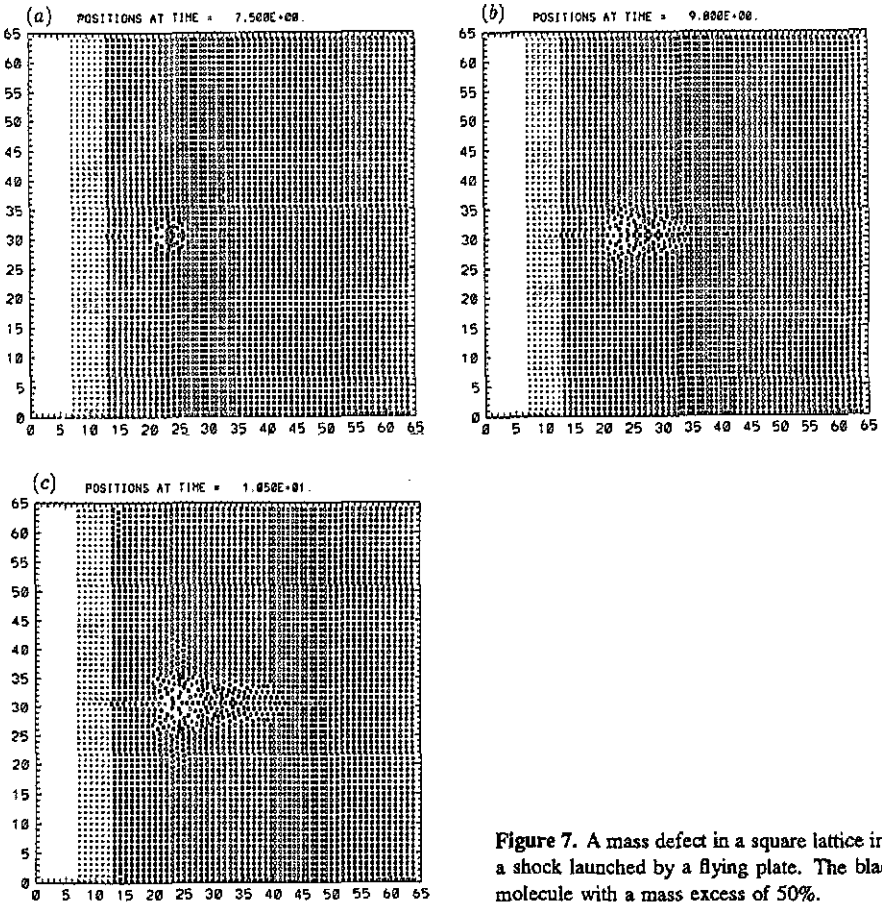

Figure 7. A mass defect in a square lattice interacting with a shock launched by a flying plate. The black square is a molecule with a mass excess of 50%.

small temperatures the perfect square lattice becomes unstable when struck by the plate, and begins to dissociate. This is true even if the potential well depth is increased by a factor of 45. The hexagonal lattice, however, is stable to impact by the flying plate over a wide range of temperatures, although at higher temperatures the shock front is less sharply defined. The effects of the various types of hexagonal lattice defects, and their relative importance, is not affected by temperature, but is strongly dependent on the intermolecular potential well depth. For a given shock strength and defect type, it appears that it is possible to increase the well depth to a point at which the lattice remains stable.

It is useful to quantify the concept of the strength of the effect of different types of lattice defects or their efficacy in disrupting the crystal when interacting with a shock. For this purpose we have defined two 'disruption factors', to be used with the two lattice symmetries. The disruption factors should be defined in such a way that the elastic deformation of the lattice due to the shock itself does not make a contribution. Therefore the disruption factors will be zero for the case of a shock traversing a defect-free crystal that remains intact.

We can define disruption factors that satisfy these criteria as follows. For the square lattice the angular positions of the four nearest neighbours ($\theta_{1,2,3,4}$) are found. The disruption factor, χ, for each particle is defined as

$$\chi = \sum_{i=1}^{4} |\sin\theta_i \cos\theta_i|$$

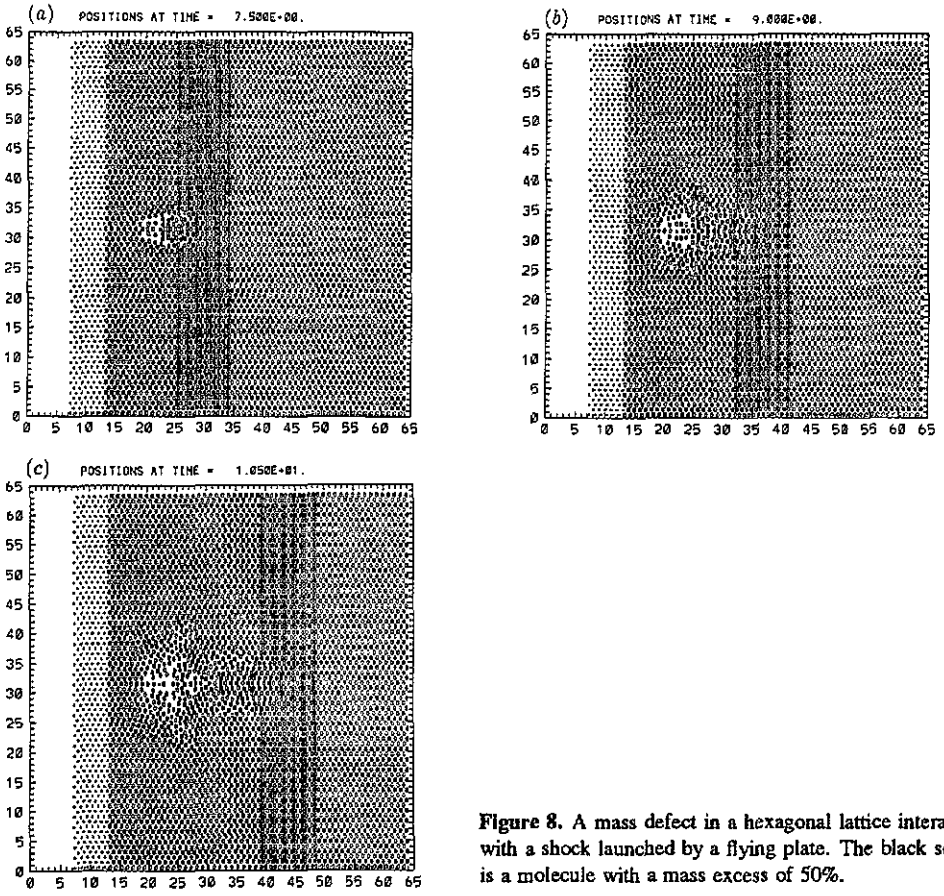

Figure 8. A mass defect in a hexagonal lattice interacting with a shock launched by a flying plate. The black square is a molecule with a mass excess of 50%.

where the summation is over near neighbours. For a compression or rarefaction of the lattice due to the propagation of a shock along one of the principal crystal axes, the angular positions of the near neighbours should remain 0, $\pm\pi/2$, and π resulting in $\chi = 0$.

The hexagonal lattice disruption factor must be defined in a slightly different manner. The angular positions of the six near neighbours of each particle ($\theta_{1\to6}$) change as the shock propagates through the lattice. In this case the angular positions of the six near neighbours are first found. The neighbours in the lower half-plane are reflected into the upper half-plane. The near neighbours are then sorted into order of increasing angle. The disruption factor for the hexagonal lattice is defined as

$$\chi = \sin\theta_1 + \sin(\theta_3 - \theta_2) + \sin(\theta_5 - \theta_4) + \sin\theta_6.$$

In the case of a shock passing through a hexagonal lattice causing only a compression or rarefaction along the shock direction, θ_1 and θ_6 should remain 0 and π, respectively. The angles θ_3 and θ_2 should be equal and θ_5 and θ_4 should be equal. As in the square lattice, a zero disruption is calculated.

The total disruption of the lattice is calculated by summing the per-particle disruption factor over all particles. The values of the total disruption correlate well with the apparent disruption found by visual inspection of the particle positions. Figures 9 and 10 display χ as a function of time for an assortment of crystal defects, for the square and hexagonal

lattices respectively. The greater importance of voids over mass defects is obvious, as is the unstable growth of the disordered region after the passage of the shock. Figure 9 also shows that the fastest growing disruption factor is found for an interstitial inclusion in a square lattice. The spatial configuration for such a system is shown in figure 11. The closer packed hexagonal lattice does not provide an equilibrium position for an interstitial inclusion.

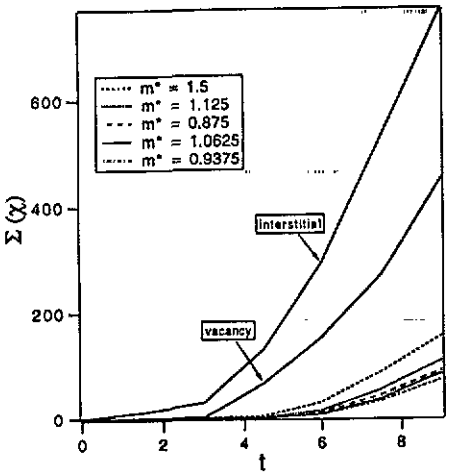

Figure 9. The disruption factor (see text) as a function of time, for several types of defects in a square lattice.

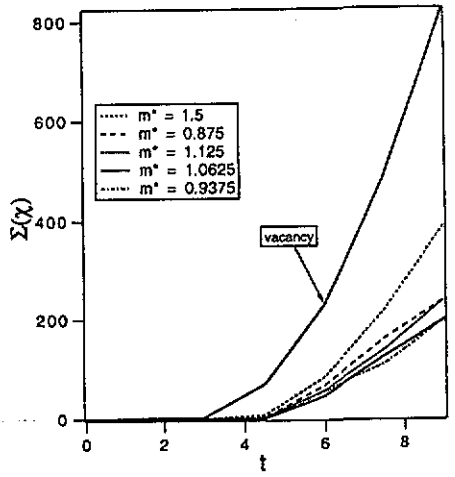

Figure 10. The disruption factor as a function of time, for mass defects of several values and for a vacancy in a hexagonal lattice.

Another useful diagnostic summary of the state of the system is a histogram distribution of the near-neighbour angular positions, such as that shown in figure 12. This figure shows the evolution of the angular distribution for the case of a vacancy in a square lattice. The additional peaks which develop in the histogram distributions indicate that the lattice is beginning to locally undergo a transition from a square to a hexagonal state. For a hexagonal lattice formed by the displacement of every other column of atoms perpendicular to the shock direction together with a compression along the shock direction, the near-neighbour angular positions should be $\pm\pi/6$, $\pm\pi/2$ and $\pm 5\pi/6$. The peaks are not found exactly at these angles since the lattice has a square structure a short distance from the region of disturbance, resulting in a distorted hexagonal state.

Figure 13 shows a calculation similar to that shown in figure 2, but in a y-periodic system of 32k molecules, with a distribution of voids whose positions, shapes and sizes (ranging from single-site vacancies to voids of nine molecules) are determined by a random number generator. This is a first attempt at simulating a system approximating a part of a real crystal, with its natural distribution of defects (although by necessity only including molecular-scale features). The basic process shown in figure 2 is repeated here: each void, including even the single-site vacancies, becomes the seed of a rapidly growing region of thermalized disorder, which causes a break in the shock front due to the work done on the voids. The shock becomes more tenuous as its organized x-momentum is equilibrated and, in the absence of energy available from chemical reactions, eventually dies out. In the second half of the figure, at $t = 11$, the leading edge of the remains of the shock front can be seen at $x = 50$. Note that for clarity only a portion of the system, which extends to $x = 260$, is shown.

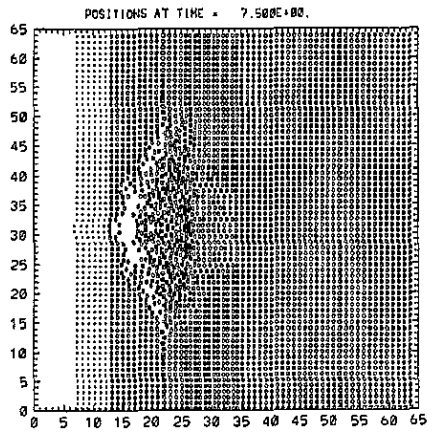

Figure 11. An interstitial inclusion in a square lattice, after the passage of a plate-launched shock.

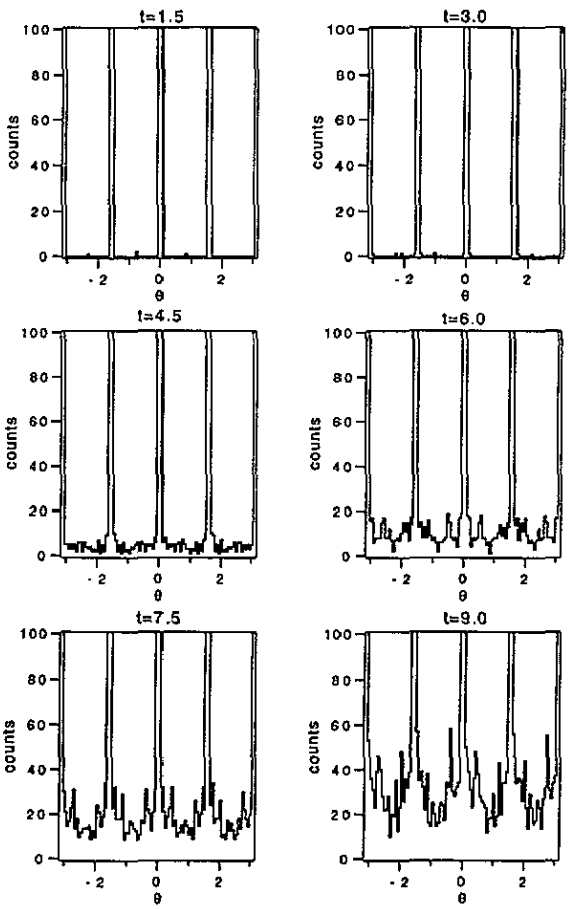

Figure 12. The evolution of the distribution of intermolecular bond angles θ in a square lattice as the shock front passes through a lattice vacancy. The set of secondary peaks that emerge in the distribution show the tendency of the lattice to relax to a locally hexagonal configuration.

The spherically symmetric potential leads to two possible periodic equilibrium lattice symmetries: square and hexagonal. As can be seen in figure 14, the agitation created by the void collapse has provided a section of the lattice the opportunity to relax to the other periodic state available to it: we see here and in various other runs the emergence of a localized hexagonal region. We use the term 'relax' above because the hexagonal state is

actually of slightly smaller potential energy. Accompanying this relaxation, therefore, must be the generation of some extra kinetic energy. A somewhat similar shock-induced phase transition was shown in [10], where a potential with two minima acted between molecules.

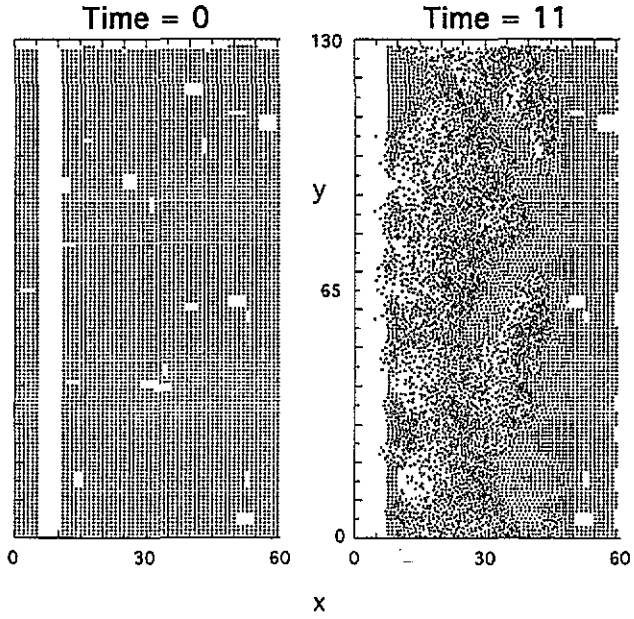

Figure 13. Particle positions in a 32k particle system, with a random distribution of voids. A flying plate has launched a shock from the left. Only a portion ($\approx$ 7.5k particles) of the total system is shown.

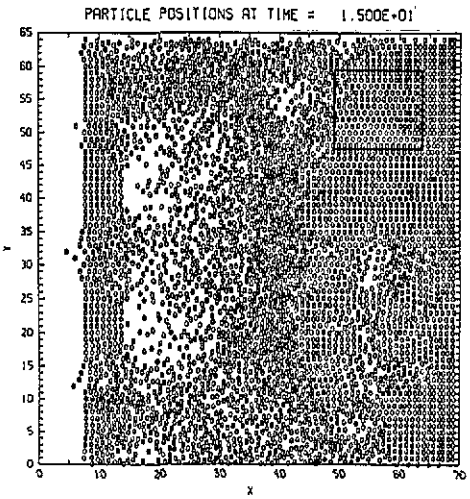

Figure 14. A frame from a later time, $t = 15$, in the calculation illustrated in figure 2, showing the emergence of an hexagonal phase embedded in the predominant square-symmetric crystal. A box has been drawn around the hexagonal region.

The assertion has been made [10] that in order to understand the shock–void interaction it is not necessary to place the void interior to the crystal but, in the interests of computational efficiency (which in this context means reducing the number of molecules that need to be tracked), it is sufficient to examine the interaction of the shock with a gap in the lattice. In figure 15 we show the results of a calculation in every way identical with that shown in figure 2, except that the two voids in figure 2 have been replaced with a gap extending

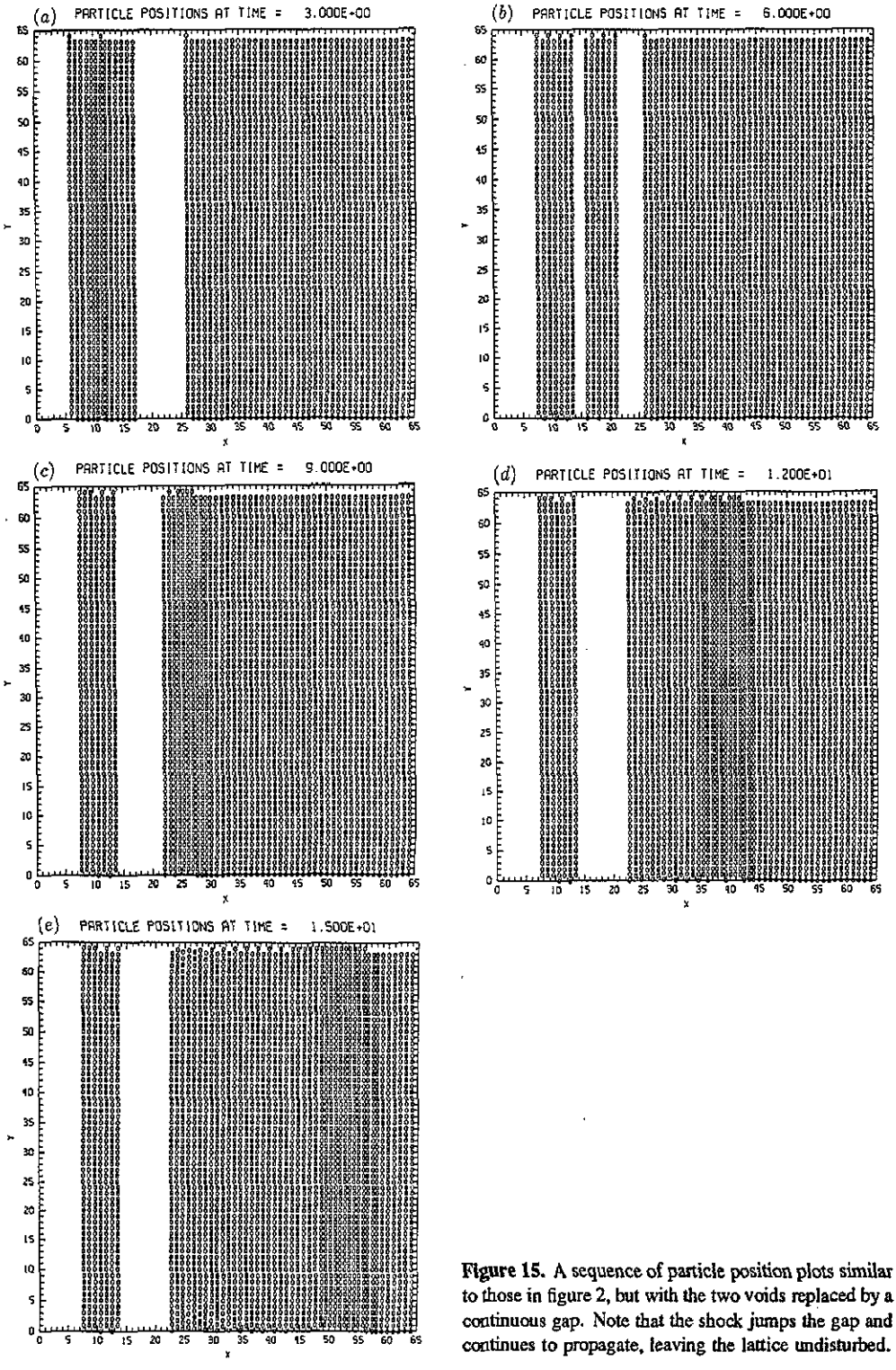

Figure 15. A sequence of particle position plots similar to those in figure 2, but with the two voids replaced by a continuous gap. Note that the shock jumps the gap and continues to propagate, leaving the lattice undisturbed.

across the entire crystal; the gap begins at the same x position as the leading edges of the voids, and has the same width. We can see from figure 15 that the shock succeeds in traversing the gap while maintaining its coherency, and procceds down the lattice, leaving it undisturbed. Thus we see an essential physical difference between a gap and an included void: the presence of neighbour molecules transverse to the direction of progress of the shock causes energy to be removed from the shock and distributed among greater degrees of freedom, leading to a thermalized region. A related observation has recently been made by Maffre and Peyrard [22], who demonstrated the ability of a shock-reaction front structure to traverse a void in a lattice.

In addition to various systems of voids, we have simulated the encounter of a shock with a type of extended defect resembling a grain boundary; the evolution of the system is shown in figure 16, which contains a sequence of plots of the particle positions in a y-periodic system. As before, a shock was launched by a flying plate travelling to the right with $V_x = 2$. At $t = 4$, the shock is beginning its traversal to the right, and the grain boundary can be seen initially at $x = 24.5$. At $t = 7$, the shock is passing over the defect, which is compressed slightly and, due to the compression of neighbouring lattice planes, has been displaced slightly to $x = 26$. At $t = 10$ the shock has passed through the defect, leaving it and the surrounding lattice undisturbed, except for coherent displacements in the x direction, which place the defect at $x = 27$. Counting from the left, the grain boundary separates the 20th from the 21st lattice plane, and it does not shift relative to the lattice. It seems likely, if these two-dimensional results are at all indicative of behaviour in three dimensions, that grain boundaries are of comparatively little importance in causing a lattice disruption, compared with voids.

There can be observed in some of the position plots a slight lack of symmetry in particle configurations where perfect symmetry might be expected, even before symmetry breaking effects have a chance to propagate in from the boundaries. The two causes for this are the small random thermal motions in the initial conditions, which are always present to some extent and are never symmetric, and the accumulated roundoff errors in the floating point arithmetic, which after a few thousand timesteps may cause a detectable breaking of symmetry even at zero temperature.

4. Conclusions

When a shock, sufficiently weak that it is able to traverse a *perfect* crystal without permanently disturbing the configuration of its lattice, encounters a void in the lattice, the void becomes the site of a rapidly growing thermalized hot fluid-like phase characterized by a high density and a high degree of collisionality. These characteristics should be conducive to the onset of chemical reactions and, we suspect, it is in these regions that the reactions leading to the development of a shock-detonation structure begin. It seems probable, therefore, that the void distribution in the lattice is an important factor controlling the sensitivity to shock-initiation and the character of the subsequent detonation front development. A perfect crystal should be relatively insensitive. It is possible that in three dimensions, other types of defects will be seen to be equally important, but that will be treated in a subsequent paper.

As discussed above, in order to concentrate on the narrowly defined problem of shocks and defects in molecular crystals, with as few complications as possible, we have deferred including a model of the chemical bond and simulated the behaviour of moderately large systems of indivisible molecules with spherically symmetrical potentials. This approach

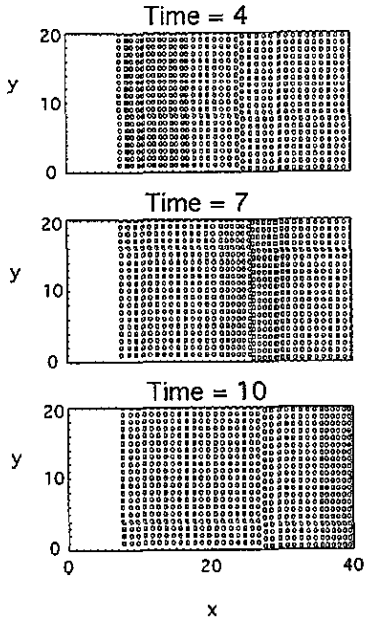

Figure 16. Particle position plot of a shock progressing through a linear defect, a vertical grain boundary initially at $x = 24.5$. At $t = 4$, the disturbance has not yet reached the defect. At $t = 7$, the disturbance is passing through the defect, and at $t = 10$ it has passed beyond the defect, leaving it undisturbed.

has the advantage that our results are independent of the details of any particular model of detonation chemistry or intramolecular behaviour, several of which are referenced in section 1.

Although we have been able to resolve several issues concerning the importance of defects, there are some remaining ambiguities that will not be resolved until we include polyatomic molecules in the simulations. These have their counterpart in the uncertainties plaguing our knowledge of the bond scission process in a shocked crystal lattice. If the polyatomic bonds are broken in the shocked region, due to direct energy transfer from the shock to vibrational modes of the molecules, then the scission forces discussed above have little relevance, because they occur in the disordered regions behind the shock. In this case the importance of the defects is in the thermalization and mixing, which will provide enhanced opportunities for the free radicals, created in the shocked region, to recombine. Of particular relevance here is the observation that thermal equilibrium is established in the disordered region close behind the shock, on a very fast timescale, implying that equilibrium equations of state may be relevant after all to the detonation process. If the chemical bonds are not broken directly by the passing shock, then the scission forces may be responsible for bond stretching and breaking in the disordered region, where conditions prevail that will enhance the subsequent reactivity. The truth is that neither computational nor theoretical work to date is sufficient to resolve these uncertainties. We hope that these questions can be addressed in the next generation of simulations, involving both defects and chemical reactions in polyatomic crystal lattices large enough to capture their interaction.

Acknowledgments

This work has benefited materially through discussions with Sam Lambrakos, Sam Trevino and Donald Tsai. It was supported by the Physics Division of the Office of Naval Research and the Naval Research Laboratory. One of us (RSS) was supported by an Office of Naval Technology postdoctoral fellowship.

References

[1] Fickett W and Davis W C 1979 *Detonation* (Berkeley, CA: University of California Press)
[2] Sandusky *et al* 1989 *Proc. 9th Int. Symp. on Detonation* p 975
[3] Dremin A N and Klimenko V Yu 1981 *Prog. Astro. Aero.* **75** 253
[4] Walker F E 1988 *LNL Report* UCRL-53860
[5] Walker F E and Wasley R J 1976 *Propellants and Explosives* **1** 73
[6] Walker F E 1982 *Propellants, Explosives and Pyrotechnics* **7** 2
[7] Walker F E 1988 *J. Appl. Phys.* **63** 5548
[8] Karo A M, Hardy J R and Walker F E 1978 *Acta Astronautica* **5** 1041
[9] Lambrakos S G, Oran E S, Boris J P and Guirguis R H 1987 *Proc. Conf. on Shock Waves in Condensed Matter* p 499
[10] Hardy J R, Karo A M and Walker F E 1981 *Gasdynamics of detonations and explosions (vol 75, Progress in Astronautics and Aeronautics)* ed J Raymond Bowen *et al* (American Institute of Aeronautics and Astronautics, Inc.) pp 209–25
[11] Karo A M, Walker F E, DeBoni T M and Hardy J R 1983 *Dynamics of Shock Waves, Explosions, and Detonations (vol 94, Progress in Astronautics and Aeronautics)* ed J Raymond Bowen *et al* (American Institute of Aeronautics and Astronautics, Inc.) pp 405–15
[12] Karo A M and Hardy J R 1986 *Int. J. Quantum Chem.* **20** 763
[13] Karo A M, Hardy J R and Mehlman M H 1986 *Proc. 15th Int. Symp. on Shock Waves and Tubes* ed D Bershader and R Hanson p 885
[14] Tsai D H and Trevino S F 1984 *J. Chem. Phys.* **81** 5636
[15] Tsai D H and Trevino S F 1983 *J. Chem. Phys.* **79** 1684
[16] Peyrard M, Odiot S, Oran E, Boris J and Schnur J 1986 *Phys. Rev.* B **33** 2350
[17] Brenner D W and White C T 1991 *Int. J. Quantum Chem.: Quantum Chem. Sym.* **23** 333
[18] Brenner D W, Elert M L and White C T 1989 *Proc. Topical Conf. on Shock Compression of Condensed Matter* p 263
[19] Elert M L, Deaven D M, Brenner D W and White C T 1989 *Phys. Rev.* B **39** 1453
[20] Lambrakos S G, Peyrard M, Oran E S and Boris J P 1990 *Phys. Rev.* B **39** 993
[21] Lambrakos S G and Peyrard M 1990 *J. Chem. Phys.* **93** 4329
[22] Maffre P and Peyrard M 1992 *Phys. Rev.* B **45** 9551
[23] Tsai D H 1991 *J. Chem. Phys.* **95** 7497
[24] Lambrakos S G and Boris J P 1987 *J. Comput. Phys.* **73** 183
[25] Memon M K, Hockney R W and Mitra S 1981 *J. Comput. Phys.* **43** 345
[26] Verlet L 1967 *PR* **159** 98
[27] Beeman D 1976 *J. Comput. Phys.* **20** 130
[28] Murray B G J P T, Bash P A and Karplus M 1988 *Thinking Machines Technical Report* CB88-3